Int. J. Solids Structures Vol. 30, No. 17, pp. 2393–2406, 1993
Printed in Great Britain

0020–7683/93 $6.00+ .00
Pergamon Press Ltd

FRACTURE MECHANICS OF ORTHOTROPIC LAMINATED PLATES—III. THE SURFACE CRACK PROBLEM

BINGHUA WU and F. ERDOGAN
Department of Mechanical Engineering, Building No. 19, Lehigh University, Bethlehem, PA 18015, U.S.A.

(*Received* 12 *March* 1992; *in revised form* 28 *September* 1992)

Abstract—In this paper the line spring model originally developed to treat the surface crack problems in homogeneous plates is extended to laminates which may consist of bonded isotropic or orthotropic dissimilar elastic layers. By using the two fundamental solutions for a laminate with a through crack and the corresponding plane strain problem for an edge crack, the surface crack problem in laminates is reduced to a system of singular integral equations. Sample results showing the stress intensity factors are given for bonded orthotropic and isotropic layers which correspond to fiber-reinforced structural composites and ceramic-coated metal substrates, respectively.

1. INTRODUCTION

In structural components which can locally be represented by a "plate" or a "shell" and which are subjected to a combination of membrane and bending loads, generally the failure process would start from a small flaw on the surface. Under cyclic loading and/or corrosion, the flaw may grow into a macroscopic surface crack. In homogeneous materials the surface crack would usually grow through the entire thickness before the final stages of failure of the component. Such subcritical crack growth processes can be monitored analytically and, consequently some statement about the service life of the component can be made, provided the surface crack solutions for the corresponding crack geometries and the baseline data for the subcritical crack propagation in the material are available (Joseph and Erdogan, 1989). The surface crack problem involved is a three-dimensional elasticity problem in which the stress field perturbed by the crack interacts very strongly with the surfaces of the component. Even in homogeneous isotropic plates the problem is much too complex to be analytically tractable. Therefore, most of the available solutions of the problem heavily rely on some kind of numerical technique such as, for example, finite elements (Newman and Raju, 1979), the alternating methods (Shah and Kobayashi, 1972; Smith and Sorensen, 1976), the boundary integral method (Heliot *et al.*, 1979; Nishioka and Atluri, 1982), the method of weight functions (Mattheck *et al.*, 1985), and the body force method (Isida *et al.*, 1984) [for reviews see Newmann (1978) and Scott and Thorpe (1981)]. However, it has also been shown that representing the medium by a "plate" or a "shell", using the concept of the "line spring model" (Rice and Levy, 1972), and by using a plate theory that accounts for transverse shear deformations, it is possible to obtain a reasonably accurate solution to the surface crack problem in plates and shells [see, for example, Joseph and Erdogan (1989) for comparison with existing finite element solutions]. In the analytical studies dealing with surface cracks for simplicity it was assumed that the plate is infinitely large. The problem of a plate with finite width containing coplanar surface cracks, including corner cracks, and subjected to remote membrane loading or bending was considered by Erdogan and Boduroglu (1984).

Up to now all existing solutions of the surface crack problems have been for homogeneous plates and shells. With the applications to composite structures and microelectronic devices and packages in mind, the primary objective of this series of papers has been to study the fracture mechanics of laminated plates which consist of bonded orthotropic layers. In this area the two physically important problems that need to be investigated are the subcritical propagation of surface cracks and the process of debonding. Only the former is addressed in this study. As indicated previously, the line spring model along with a shear

deformation plate theory provides a relatively simple and effective technique for solving the surface crack problem in homogeneous and isotropic plates and shells. The effect of material orthotropy in homogeneous plates was considered by Wu and Erdogan (1989). The technique was extended to the case of plates containing multiple surface or embedded cracks by Erdogan and Aksel (1988). In this paper the problem of a surface crack in laminated orthotropic plates is considered. The two fundamental problems necessary for the application of the line spring model were discussed in Parts I and II of this paper. These were the through crack problem in orthotropic laminates under membrane and bending loads and the edge crack problem in bonded orthotropic layers under plane strain conditions. As explained in Part II, in this paper, too, the analysis will be confined to plates that consist of only two layers. If the laminates contain more than two layers, then it is assumed that the two parts of the plate on either side of the interface of primary interest are properly homogenized as separate orthotropic layers.

2. THE LINE SPRING MODEL

In a relatively thin-walled plate or shell structure containing a surface crack and subjected to membrane and bending loads, the "net ligament" around the part-through crack would generally have a constraining effect on the crack surface displacements. Thus, the basic idea underlying the line spring model consists of approximating the inherently three-dimensional surface crack problem by a two-dimensional coupled membrane-bending plate or shell problem through the reduction of net ligament stresses [Fig. 1(a)] to the neutral surface of the plate or the shell as a membrane load N and a bending moment M [Fig. 1(b)] (Rice and Levy, 1972). The problem shown in Fig. 1(a) is, thus, reduced to a plate bending problem for a through crack described in Fig. 1(b) with unknown membrane and bending resultants N and M acting on the crack surface. In the plate bending problem the crack surface displacements are represented by a crack opening displacement δ and a crack surface rotation θ measured, again, at the neutral surface. Note that the quantities N, M, δ and θ are all unknown and are functions of y only [Fig. 1(b)]. In the coupled case the mixed boundary value problem for a plate containing a through crack is formulated in terms of a system of integral equations with, essentially, $\delta(y)$ and $\theta(y)$ as the unknown functions. In the current problem there are, however, two more unknown functions, $N(y)$ and $M(y)$ which appear in the formulation as "crack surface tractions", that is as a

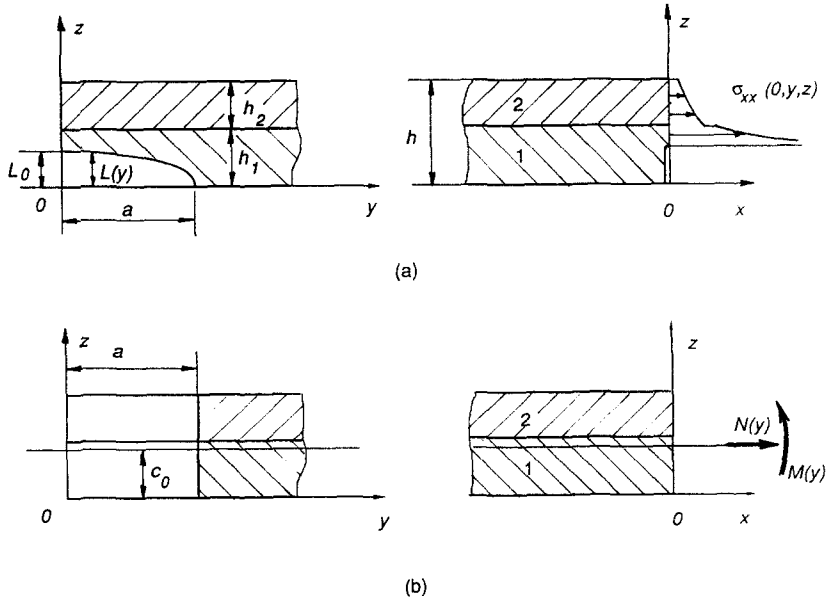

Fig. 1. Geometry of the laminated plate with a surface crack; (a) the part-through crack, (b) the line-spring approximation.

component of the input functions. Therefore, aside from the integral equations, two more relations between the complementary quantities (δ, θ) and (N, M) are needed to complete the formulation. These relations are obtained by using energy considerations.

As was the case in the bending problem of plates with a through crack, the early applications of the line spring model, too, were based on the classical plate theory. Aside from the motivation for obtaining more accurate results for the stress intensity factors, there appear to be also conceptual reasons for using a higher order plate theory which can accommodate all boundary conditions on the crack surfaces separately rather than lumping the transverse shear resultant with the twisting moment. The asymptotic stress field around the crack tip given by the classical plate bending theory is not consistent with continuum elasticity results (with regard to the angular distribution of stresses, dependence on Poisson's ratio, and the power of singularity in transverse shear stresses), whereas a shear deformation theory gives results which are identical to the asymptotic solutions obtained from the plane strain and antiplane shear problems (Knowles and Wang, 1960; Yahsi and Erdogan, 1979). The question of accuracy of the asymptotic results for very thin plates has been resolved by determining the limit of the stress intensity factor analytically (Joseph and Erdogan, 1991a).

Consider now the general membrane/bending problem for an orthotropic laminate containing a through crack [Fig. 1(b)]. The corresponding perturbation problem in which the crack surface tractions are the only nonzero applied loads must be solved under the following boundary conditions:

$$N_{xy}(0, y) = 0, \quad M_{xy}(0, y) = 0, \quad Q_x(0, y) = 0, \quad -\infty < y < \infty, \tag{1}$$

$$N_{xx}(0, y) = hf_1(y), \quad |y| < a,$$
$$u_0(0, y) = 0, \quad -\infty < y < -a, \quad a < y < \infty, \tag{2}$$

$$M_{xx}(0, y) = (h^2/6)f_2(y), \quad |y| < a,$$
$$\psi_x(0, y) = 0, \quad -\infty < y < -a, \quad a < y < \infty, \tag{3}$$

where, in the usual notation, N_{ij}, M_{ij} and Q_i, $(i, j = x, y)$ are, respectively, the stress, moment and transverse shear resultants, u_0 is the in-plane component of the displacement at the reference plane (in this case assumed to be the neutral plane), ψ_x is the rotation of the normal to the neutral plane, and f_1 and f_2 are arbitrary crack surface tractions [see Wu (1990) for details]. If we define

$$\frac{\partial}{\partial y}u_0(0, y) = g_1(y), \quad \frac{\partial}{\partial y}\psi_x(0, y) = g_2(y), \tag{4}$$

it was shown by Wu (1990) that, by using a first order shear deformation theory, the related mixed boundary value problem may be reduced to a system of integral equations of the form

$$\sum_{j=1}^{2}\int_{-a}^{a}\left[\frac{1}{\pi}\frac{\mu_{kj}}{t-y} + k_{kj}(y, t)\right]g_j(t)\,dt = f_k(y), \quad k = 1, 2, |y| < a, \tag{5}$$

subject to

$$\int_{-a}^{a} g_j(t)\,dt = 0, \quad j = 1, 2, \tag{6}$$

where μ_{kj} are known material constants and the kernels k_{kj} are known functions.

In the perturbation problem simulating the part-through crack in a laminate subjected to remote membrane loading $N_{xx} = N_0$ and bending $M_{xx} = M_0$, the crack surface tractions may be expressed as

$$\begin{aligned} hf_1(y) &= -N_0 + N(y), \\ \frac{h^2}{6} f_2(y) &= -M_0 + M(y), \quad -a < y < a, \end{aligned} \tag{7}$$

where the assumption is that the resultants N and M are statically equivalent to and represent the net ligament stress $\sigma_{xx}(0, y, z)$, $(-a < y < a, L(y) < z < h)$. Note that N and M tend to close the crack surfaces whereas the external loads N_0 and M_0 tend to open them. The second major assumption in developing the model is that the stress intensity factor at a location y along the crack front may locally be approximated by the corresponding plane strain value obtained from a laminate which contains an edge crack of depth $L(y)$ and which is subjected to uniform membrane loading N and bending moment M. This assumption makes it possible to express N and M in terms of the displacement quantities g_1 and g_2. In order to determine these relationships, the energy available for fracture along the crack front is expressed in two different ways, namely as the crack closure energy and as the product of load and load point displacement. Thus, if $k_1(y)$ is the mode I stress intensity factor along the crack front, the strain energy release rate or the energy available for fracture may be expressed as

$$\mathcal{G} = \frac{\partial}{\partial L}(U - V) = \frac{\pi k_1^2}{2\mu^*}, \tag{8}$$

where U is the work done by the external loads, V is the strain energy and for the plane strain case under consideration the material constant μ^* is defined by

$$\mu^* = \frac{1}{2}\left(\frac{d_{11}d_{33}}{2}\right)^{-1/2}\left[\left(\frac{d_{11}}{d_{33}}\right)^{1/2} + \frac{2d_{13} + d_{55}}{2d_{33}}\right]^{-1/2},$$

$$d_{11} = \frac{c_{11}c_{22} - c_{12}^2}{c_{22}}, \quad d_{33} = \frac{c_{33}c_{22} - c_{23}^2}{c_{22}}, \tag{9}$$

$$d_{13} = \frac{c_{13}c_{22} - c_{12}c_{32}}{c_{22}}, \quad d_{55} = c_{55}, \tag{10}$$

c_{ij}, $(i, j = 1, 2, 3$ or $x, y, z)$, being the coefficients of the compliance matrix c (in $\varepsilon = c\sigma$) in the orthotropic layer 1 which contains the crack (Wu, 1990, Fig. 1). Note that in isotropic materials

$$\mu^* = 4\mu/(1 + \kappa) = E/2(1 - \nu^2). \tag{11}$$

The work done by N and M through "load point displacements" $d\delta$ and $d\theta$ (which results from the crack growth dL) minus the strain energy stored, that is, the energy available for fracture, may also be expressed as

$$d(U - V) = \tfrac{1}{2}(Nd\delta + Md\theta). \tag{12}$$

Thus, from (12), (8) and

$$d\delta = \frac{\partial \delta}{\partial L} dL, \quad d\theta = \frac{\partial \theta}{\partial L} dL, \tag{13}$$

it follows that

$$\frac{\partial}{\partial L}(U-V) = \mathcal{G} = \tfrac{1}{2}\left(N\frac{\partial \delta}{\partial L} + M\frac{\partial \theta}{\partial L}\right) = \frac{\pi k_1^2}{2\mu^*}. \tag{14}$$

Referring to Part II of this study from the plane strain crack solution k_1 may be obtained as

$$k_1(b) = \sqrt{h}\left[\frac{N}{h} g_t(s) + \frac{M}{h^2/6} g_b(s)\right], \quad s = L/h. \tag{15}$$

If we now define the matrices

$$\tau = \begin{bmatrix} N/h \\ 6M/h^2 \end{bmatrix}, \quad \omega = \begin{bmatrix} \delta \\ h\theta/6 \end{bmatrix}, \quad G(s) = \begin{bmatrix} g_t^2 & g_t g_b \\ g_t g_b & g_b^2 \end{bmatrix}, \tag{16}$$

(14) becomes

$$\frac{\pi h}{2\mu^*} \tau^{\mathrm{T}} G \tau = \frac{h}{2} \tau^{\mathrm{T}} \frac{\partial \omega}{\partial L}, \tag{17}$$

giving

$$\frac{\partial \omega}{\partial L} = \frac{\pi}{\mu^*} G\tau. \tag{18}$$

Observing that G is a function of $s = L/h$, τ is independent of L and $\omega = 0$ for $L = 0$, from (18) we find

$$\omega = \frac{h\pi}{\mu^*} A\tau, \quad A = \frac{1}{h}\int_0^L G(L/h)\,\mathrm{d}L = \int_0^s G(s)\,\mathrm{d}s. \tag{19}$$

From (16), (19) and (15) it may now easily be seen that

$$\begin{aligned} \frac{N}{h} &= \frac{\mu^*}{\pi h}\left[2\alpha_{11}\int_{-a}^{y} g_1(t)\,\mathrm{d}t + \frac{h}{3}\alpha_{12}\int_{-a}^{y} g_2(t)\,\mathrm{d}t\right], \\ \frac{M}{h^2/6} &= \frac{\mu^*}{\pi h}\left[2\alpha_{21}\int_{-a}^{y} g_1(t)\,\mathrm{d}t + \frac{h}{3}\alpha_{22}\int_{-a}^{y} g_2(t)\,\mathrm{d}t\right], \end{aligned} \tag{20}$$

where the matrix (α_{ij}) is given by

$$(\alpha_{ij}) = \alpha = A^{-1}. \tag{21}$$

Note that α_{ij} are dimensionless and are functions of $s = L(y)/h$. Finally, by substituting from (7) and (20) into (5) we obtain

$$\int_{-a}^{a}\left[\frac{1}{\pi}\frac{\mu_{11}}{t-y}+k_{11}(y,t)\right]g_1(t)\,dt+\int_{-a}^{a}\left[\frac{1}{\pi}\frac{\mu_{12}}{t-y}+k_{12}(y,t)\right]g_2(t)\,dt$$
$$-\frac{\mu^*}{\pi h}\left[2\alpha_{11}\int_{-a}^{y}g_1(t)\,dt+\frac{h}{3}\alpha_{12}\int_{-a}^{y}g_2(t)\,dt\right]=-\frac{N_0}{h},\quad -a<y<a,$$
$$\int_{-a}^{a}\left[\frac{1}{\pi}\frac{\mu_{21}}{t-y}+k_{21}(y,t)\right]g_1(t)\,dt+\int_{-a}^{a}\left[\frac{1}{\pi}\frac{\mu_{22}}{t-y}+k_{22}(y,t)\right]g_2(t)\,dt$$
$$-\frac{\mu^*}{\pi h}\left[2\alpha_{21}\int_{-a}^{y}g_1(t)\,dt+\frac{h}{3}\alpha_{22}\int_{-a}^{y}g_2(t)\,dt\right]=-\frac{6M_0}{h^2},\quad -a<y<a. \tag{22}$$

After determining g_1 and g_2 from (22), (20) gives $N(y)$ and $M(y)$ and $k_1(y)$ may be obtained from (15).

The "shape functions" g_t and g_b defining the stress intensity factor in (15) are obtained by solving the corresponding plane strain edge crack problem described in Part II of this study and may be expressed as follows:

$$g_t(s)=\sqrt{s}\sum_{k=0}^{n}a_{tk}s^k,\quad g_b(s)=\sqrt{s}\sum_{k=0}^{n}a_{bk}s^k,\quad s=L/h. \tag{23}$$

The solution of (22) is obtained by letting

$$g_j(t)=F_j(t)/\sqrt{a^2-t^2},\quad j=1,2, \tag{24}$$

and by following the procedure described in, for example, Erdogan (1978).

3. THE RESULTS AND DISCUSSION

The line spring model described in this paper is known to provide a relatively simple approximation to the three-dimensional elasticity problem in a plate or a shell containing a surface crack. Comparisons of the stress intensity factors obtained from the line spring model and that given by the existing finite element solutions indicate that the differences are rather insignificant. An example showing the calculated stress intensity factors in a homogeneous isotropic plate containing a semi-elliptic surface crack of length $2a$ and depth L_0 (Fig. 1) and subjected to remote tension or bending is given in Fig. 2. The results are

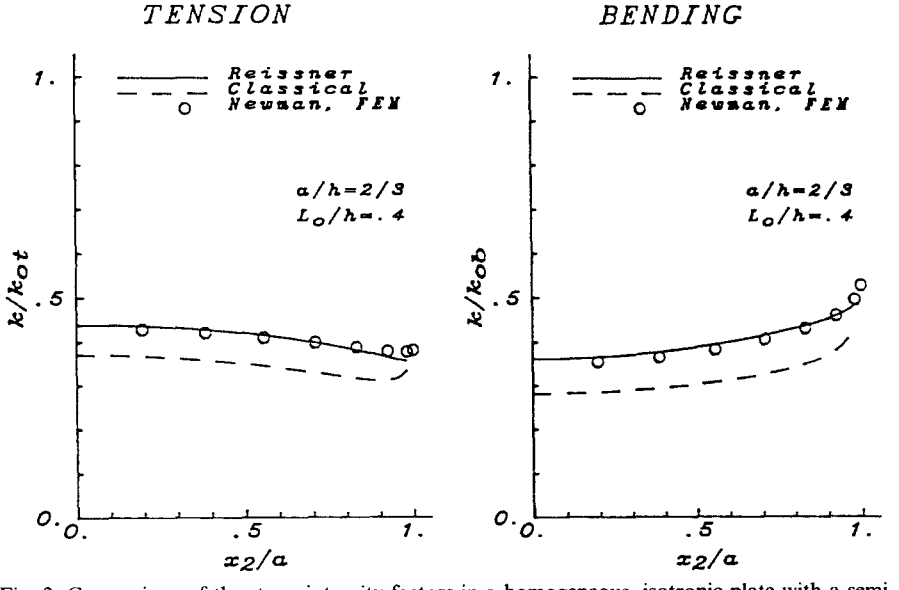

Fig. 2. Comparison of the stress intensity factors in a homogeneous, isotropic plate with a semi-elliptic surface crack obtained from the finite element solution (Newman and Raju, 1979) and the line spring model using the classical plate theory and the Reissner theory (Joseph and Erdogan, 1989), $\nu=0.3$, $a/h=(2/3)$.

obtained by Newman and Raju (1979) using a finite element method and by Joseph and Erdogan (1989) the line spring model in conjunction with the classical plate theory and the Reissner theory. The figure shows that the results of the shear deformation theory agree rather well with the finite element solution. Further comparison of stress intensity factors in homogeneous plates containing a part-through crack of various geometries may be found in Joseph and Erdogan (1989) and Erdogan and Aksel (1988) for mode I and in Joseph and Erdogan (1991b) for mixed mode loading conditions.

The elastic constants of the materials used in the examples considered in this section are given in Table 1. Materials 1 and 2 are fiber-reinforced composites (graphite-epoxy) which are orthotropic and are widely used in structural applications. The remaining three materials are isotropic; material 3 is steel, 4 is zirconia, and 5 is alumina. Table 2 shows the material combinations used in two layer laminates considered in the numerical examples. Note that, except for a 90° material rotation about the z-axis, materials 1 and 2 are identical. Thus the difference between the material pairs A and B is simply the crack orientation. Material pairs C and D are included because of their relevance to surface cracking of ceramic coatings on metal substrates.

Some sample results showing the stress intensity factors in two bonded layers containing an edge crack of depth L obtained from the plane strain elasticity solution are given in Tables 3 and 4. Referring to (15), k_{1t} and k_{1b} shown in these tables are related to the shape functions g_t and g_b by

Table 1. The elastic constants of materials used in the example (all in units of GPA)

Material 1	Material 2	Material 3	Material 4	Material 5
$E_x = 39$	$E_x = 30.6$	$E = 200$	$E = 137.9$	$E = 325$
$E_y = 30.6$	$E_x = 39$	$\nu = 0.26$	$\nu = 0.26$	$\nu = 0.3$
$E_z = 6.4$	$E_z = 6.4$			
$G_{xy} = 19.7$	$G_{xy} = 19.7$			
$G_{yz} = 4.5$	$G_{yz} = 4.5$			
$G_{xz} = 4.5$	$G_{xz} = 4.5$			
$\nu_{xy} = 0.447$	$\nu_{xy} = 0.351$			
$\nu_{xz} = 0.275$	$\nu_{xz} = 0.275$			
$\nu_{yz} = 0.275$	$\nu_{yz} = 0.275$			

Table 2. Material combinations used in the examples

Material Pair	Layer 1	Layer 2
A	2	1
B	1	2
C	5	3
D	4	3
I	3	3

Table 3. Normalized stress intensity factors in two bonded orthotropic layers containing an edge crack and subjected to remote membrane loading N_0 or bending M_0 under plane strain conditions; Fig. 1, $\sigma_t = N_0/h$, $\sigma_b = 6M_0/h^2$, Material Pair B

	$h_2/h_1 = 10$		$h_2/h_1 = 1$		$h_2/h_1 = 0.1$	
L/h_1	$k_{1t}/\sigma_t\sqrt{L}$	$k_{1b}/\sigma_b\sqrt{L}$	$k_{1t}/\sigma_t\sqrt{L}$	$k_{1b}/\sigma_b\sqrt{L}$	$k_{1t}/\sigma_t\sqrt{L}$	$k_{1b}/\sigma_b\sqrt{L}$
0.001	1.100	1.100	1.100	1.100	1.100	1.100
0.1	1.060	1.003	1.120	1.050	1.192	1.004
0.2	1.000	0.984	1.164	1.016	1.298	1.021
0.3	1.031	0.985	1.248	1.016	1.545	1.077
0.4	1.036	0.988	1.355	1.028	1.904	1.178
0.5	1.054	0.993	1.492	1.055	2.436	1.344
0.6	1.073	1.000	1.664	1.097	3.254	1.609
0.7	1.094	1.007	1.881	1.157	4.591	2.046
0.8	1.117	1.016	2.160	1.243	6.949	2.803
0.9	1.143	1.027	2.538	1.368	11.342	4.126

Table 4. Same as Table 3, Material Pair D

	$h_2/h_1 = 5$		$h_2/h_1 = 1$		$h_2/h_1 = 0.2$	
L/h_1	$k_{1t}/\sigma_t\sqrt{L}$	$k_{1b}/\sigma_b\sqrt{L}$	$k_{1t}/\sigma_t\sqrt{L}$	$k_{1b}/\sigma_b\sqrt{L}$	$k_{1t}/\sigma_t\sqrt{L}$	$k_{1b}/\sigma_b\sqrt{L}$
0.001	1.1215	1.1215	1.1215	1.1215	1.1215	1.1215
0.1	1.119	1.074	1.132	1.070	1.161	1.052
0.2	1.114	1.072	1.171	1.044	1.278	1.045
0.3	1.113	1.049	1.234	1.036	1.464	1.081
0.4	1.113	1.027	1.319	1.043	1.734	1.158
0.5	1.114	1.007	1.426	1.062	2.119	1.284
0.6	1.114	0.987	1.556	1.091	2.677	1.480
0.7	1.112	0.967	1.709	1.130	3.522	1.785
0.8	1.109	0.944	1.882	1.174	4.874	2.277
0.9	1.104	0.914	2.058	1.212	7.147	3.093

$$k_{1t}(L) = \frac{N_0}{h}\sqrt{h}g_t(s), \quad k_{1b}(L) = \frac{6M_0}{h^2}\sqrt{h}g_b(s), \quad s = L/h. \tag{25}$$

Results such as those given in Tables 3 and 4 are used to calculate the coefficients a_{tk} and a_{bk} of the shape functions defined in (23). Sample results for typical material pairs showing these coefficients are given in Tables 5 and 6. After tabulating $g_t(s)$ and $g_b(s)$, a_{tk} and a_{bk} are obtained through a curve-fitting process by expressing

$$g_b(s) = \sqrt{s}\sum_0^n a_{bk}s^k, \tag{26}$$

$$g_t(s) = \sqrt{s}\sum_0^n a_{tk}s^{2k}, \quad h_2/h_1 \leqslant 1, \tag{27}$$

$$g_t(s) = \sqrt{s}\sum_0^n a_{tk}s^k, \quad h_2/h_1 > 1. \tag{28}$$

Table 5. The coefficients a_{tk} and a_{bk} for the shape functions g_t and g_b giving the stress intensity factor in a two layer laminate subjected to remote membrane loading N_0 or bending M_0 under plane strain conditions [see eqns (15) and (23)], orthotropic layers, Material Pairs A and B

	Material Pair A		Material Pair B					
	$h_2/h_1 = 1$		$h_2/h_1 = 10$		$h_2/h_1 = 1$		$h_2/h_1 = 0.1$	
k	a_{tk}	a_{bk}	a_{tk}	a_{bk}	a_{tk}	a_{bk}	a_{tk}	a_{bk}
0	1.103	1.107	1.019	1.033	1.101	1.102	1.107	1.102
1	6.172	−1.278	17.083	−2.537	6.637	−1.499	5.837	−2.159
2	−13.434	6.195	24.226	19.186	−9.789	8.323	−4.321	16.133
3	90.976	−7.717			64.081	−17.56	50.836	−53.66
4	−196.82	5.208			−22.36	20.85	−116.96	108.8
5							180.96	−112.5
6							−87.04	52.913

Table 6. Same as Table 5, Material Pairs C and D

	Material Pair C				Material Pair D			
	$h_2/h_1 = 5$		$h_2/h_1 = 1$		$h_2/h_1 = 5$		$h_2/h_1 = 1$	
k	a_{tk}	a_{bk}	a_{tk}	a_{bk}	a_{tk}	a_{bk}	a_{tk}	a_{bk}
0	1.019	1.110	1.121	1.121	1.120	1.116	1.12	1.120
1	0.528	−0.901	7.786	−1.672	−0.333	−1.732	5.25	−1.189
2	15.81	8.284	−12.31	10.71	4.849	9.058	−8.925	4.565
3	−5.67	23.269	78.050	−26.47	−22.62	−42.95	66.168	−2.533
4			43.543	33.67			−183.23	−1.605

One of the advantages of the technique described in this paper is that it can be used to determine the stress intensity factors for surface cracks of any given profile. This, of course, simplifies quite considerably the process of monitoring the subcritical crack growth (Joseph and Erdogan, 1989). The results in this paper are, however, given for only two crack profiles, namely semi-elliptic and rectangular. In the case of the semi-elliptic surface crack $L(y)$ is given by (see Fig. 1)

$$L(y) = L_0\sqrt{1-(y/a)^2}, \tag{29}$$

whereas in the rectangular crack $L(y) = L_0$, $-a < y < a$.

Table 7 shows some results for the normalized stress intensity factors at the maximum penetration point $L = L_0$ of a semi-elliptic surface crack in orthotropic laminates under remote membrane loading $N_{xx} = N_0$ or bending $M_{xx} = M_0$. In this table the normalizing stress intensity factors k_{0t} and k_{0b} are the corresponding plane strain values obtained from the edge crack solution and are the limits of $k_t(0)$ and $k_b(0)$ for $a \to \infty$. Thus, referring to (25) k_{0t} and k_{0b} may be obtained from

$$k_{0t}(L) = \frac{N_0}{h}\sqrt{h}g_t(s_0), \quad k_{0b}(L) = \frac{6M_0}{h^2}\sqrt{h}g_b(s_0), \quad s_0 = L_0/h. \tag{30}$$

$k_t(y)$ and $k_b(y)$ shown in Table 7 and in the subsequent tables given in this paper are the actual mode I stress intensity factors at the location y along the crack front due to the

Table 7. Normalized stress intensity factors at the center ($L(0) = L_0$) of a semi-elliptic surface crack in a two layer orthotropic laminate subjected to remote membrane loading N_0 and bending M_0; $\bar{k}_t = k_t(0)/k_{0t}$, $\bar{k}_b = k_b(0)/k_{0b}$

$L_0/h_1 =$	0.3		0.6		0.9	
a/h	$\bar{k}_t$	$\bar{k}_b$	$\bar{k}_t$	$\bar{k}_b$	$\bar{k}_t$	$\bar{k}_b$
	Material Pair A, $h_2/h_1 = 1$					
6	0.955	0.954	0.821	0.806	0.637	0.591
4	0.936	0.934	0.768	0.747	0.563	0.506
2	0.892	0.888	0.663	0.631	0.442	0.365
1	0.829	0.821	0.546	0.500	0.333	0.238
0.5	0.736	0.723	0.419	0.358	0.255	0.130
0.25	0.607	0.586	0.299	0.223	0.179	0.050
	Material Pair B, $h_2/h_1 = 1$					
6	0.961	0.960	0.840	0.824	0.648	0.601
4	0.944	0.942	0.790	0.768	0.575	0.515
2	0.904	0.899	0.688	0.653	0.451	0.369
1	0.843	0.835	0.568	0.518	0.337	0.234
0.5	0.751	0.738	0.437	0.368	0.241	0.121
0.25	0.586	0.601	0.312	0.225	0.169	0.038
	Material Pair B, $h_2/h_1 = 10$					
6	0.996	0.996	0.988	0.992	0.968	0.981
4	0.995	0.996	0.984	0.989	0.956	0.974
2	0.993	0.994	0.973	0.981	0.928	0.955
1	0.990	0.991	0.957	0.969	0.885	0.924
0.5	0.984	0.986	0.927	0.946	0.813	0.872
0.25	0.971	0.975	0.872	0.905	0.691	0.794
	Material Pair B, $h_2/h_1 = 0.1$					
6	0.862	0.852	0.503	0.432	0.137	0.034
4	0.817	0.802	0.430	0.345	0.112	0.007
2	0.722	0.699	0.320	0.215	0.078	−0.024
1	0.609	0.573	0.231	0.111	0.054	−0.041
0.5	0.477	0.428	0.163	0.033	0.037	−0.043

external loads N_0 and M_0, respectively. Some surface crack results for isotropic material pairs corresponding to a ceramic coating with a smaller (pair C) and a greater (pair D) stiffness than that of the metal substrate are shown in Table 8. The results shown in this table are self-explanatory and conform to expected physical trends and analytical limits.

Sample results showing the variation of the stress intensity factors along the crack front in laminates with a semi-elliptic or a rectangular surface crack are given in Table 9. Table 10 shows the influence of the thickness ratio h_2/h_1 as well as the crack depth L_0 on the stress intensity factors in a ceramic-metal pair.

The effect of the crack length on the normalized stress intensity factors in a two layer bonded orthotropic laminate (Material Pair B) containing a semi-elliptic surface crack is shown in Figs 3 and 4 for membrane loading and bending, respectively. For reference, similar results are also shown in Figs 5 and 6 for an isotropic plate (Material Pair I). The normalizing stress intensity factors k_{0t} and k_{0b} used in these figures are the corresponding plane strain values given by (30). The stress intensity factor k shown in these figures is calculated at the maximum penetration point $L = L_0$ of the semi-elliptic surface crack and is $k_t(0)$ or $k_b(0)$ shown in Tables 7–10. Comparison of the results given in Figs 3 and 5, and 4 and 6 would show that the stress intensity factors in the particular orthotropic material (pair B) under consideration are consistently lower than the values computed for the homogeneous isotropic plate (Material Pair I). This may also be seen from Fig. 7 where the stress intensity factor is normalized with respect to a fixed value, $k_{0t} = (N_0/h)\sqrt{h_1}$. Note that in all cases, the limiting values of the calculated results are

$$\lim_{a\to\infty}[k(L_0)/k_{0t}] = 1, \quad \lim_{a\to 0}[k(L_0)/k_{0t}] = 0. \tag{31}$$

Table 8. Same as Table 7, Material Pairs C and D

L_0/h_1 =	0.3		0.6		0.9	
a/h	$\bar{k}_t$	$\bar{k}_b$	$\bar{k}_t$	$\bar{k}_b$	$\bar{k}_t$	$\bar{k}_b$
	Material Pair C, $h_2/h_1 = 1$					
6	0.972	0.974	0.897	0.900	0.747	0.739
4	0.960	0.964	0.857	0.861	0.674	0.663
2	0.931	0.938	0.767	0.775	0.538	0.523
1	0.887	0.899	0.653	0.669	0.404	0.390
0.5	0.818	0.843	0.520	0.549	0.281	0.273
	Material Pair C, $h_2/h_1 = 5$					
6	1.003	1.003	0.995	0.996	0.979	0.979
4	1.001	1.002	0.991	0.991	0.968	0.967
2	0.998	0.999	0.979	0.978	0.940	0.938
1	0.994	0.994	0.961	0.960	0.900	0.896
0.5	0.986	0.986	0.932	0.930	0.840	0.834
0.25	0.972	0.972	0.883	0.879	0.750	0.740
	Material Pair D, $h_2/h_1 = 1$					
6	0.959	0.962	0.856	0.863	0.707	0.706
4	0.942	0.946	0.804	0.813	0.627	0.624
2	0.899	0.909	0.693	0.709	0.483	0.481
1	0.836	0.855	0.563	0.591	0.348	0.353
0.5	0.747	0.782	0.424	0.468	0.262	0.246
	Material Pair D, $h_2/h_1 = 5$					
6	0.993	0.993	0.981	0.981	0.965	0.964
4	0.991	0.991	0.974	0.973	0.950	0.949
2	0.986	0.985	0.954	0.954	0.913	0.911
1	0.977	0.977	0.926	0.925	0.862	0.858
0.5	0.944	0.964	0.883	0.882	0.791	0.784
0.25	0.940	0.939	0.815	0.813	0.689	0.677

Table 9. Variation of stress intensity factor along the crack front in a two layer laminate containing a semi-elliptic, or a rectangular surface crack and subjected to remote membrane loading N_0 or bending M_0; $\bar{k}_t = k_t(y)/k_{0t}$, $\bar{k}_b = k_b(y)/k_{0b}$, Material Pair B, $h_2/h_1 = 1$, $a/h = 1$

$L_0/h_1 =$	0.3		0.6		0.9	
y/a	$\bar{k}_t$	$\bar{k}_b$	$\bar{k}_t$	$\bar{k}_b$	$\bar{k}_t$	$\bar{k}_b$
	Semi-elliptic surface crack					
0.0	0.843	0.835	0.568	0.518	0.337	0.234
0.1	0.838	0.831	0.566	0.516	0.336	0.235
0.2	0.827	0.821	0.559	0.515	0.333	0.237
0.3	0.814	0.812	0.553	0.514	0.328	0.243
0.4	0.803	0.809	0.547	0.521	0.324	0.253
0.5	0.793	0.808	0.542	0.532	0.320	0.267
0.6	0.774	0.801	0.532	0.542	0.314	0.283
0.7	0.732	0.771	0.512	0.544	0.304	0.299
0.8	0.667	0.717	0.483	0.545	0.292	0.318
0.9	0.616	0.685	0.463	0.557	0.284	0.351
	Rectangular surface crack					
0.0	0.891	0.876	0.627	0.563	0.376	0.258
0.1	0.886	0.874	0.622	0.563	0.373	0.257
0.2	0.875	0.870	0.610	0.562	0.364	0.257
0.3	0.866	0.863	0.598	0.556	0.355	0.254
0.4	0.863	0.857	0.589	0.540	0.348	0.241
0.5	0.862	0.848	0.581	0.515	0.342	0.222
0.6	0.850	0.831	0.561	0.485	0.329	0.199
0.7	0.814	0.799	0.518	0.450	0.301	0.179
0.8	0.752	0.745	0.453	0.398	0.261	0.151
0.9	0.662	0.635	0.380	0.289	0.222	0.086

Table 10. Same as Table 9, semi-elliptic surface crack in a laminate of Material Pair C, $a/h = 1$

$L_0/h_1 =$	0.3		0.6		0.9	
y/a	$\bar{k}_t$	$\bar{k}_b$	$\bar{k}_t$	$\bar{k}_b$	$\bar{k}_t$	$\bar{k}_b$
	$h_2/h_1 = 1$					
0.0	0.887	0.899	0.653	0.669	0.404	0.390
0.1	0.885	0.899	0.652	0.670	0.403	0.391
0.2	0.881	0.897	0.650	0.672	0.401	0.395
0.3	0.871	0.891	0.643	0.672	0.396	0.399
0.4	0.852	0.879	0.632	0.670	0.388	0.403
0.5	0.826	0.859	0.614	0.664	0.377	0.407
0.6	0.792	0.834	0.593	0.657	0.365	0.411
0.7	0.754	0.806	0.571	0.652	0.353	0.420
0.8	0.704	0.767	0.542	0.643	0.341	0.431
0.9	0.603	0.673	0.481	0.597	0.315	0.427
	$h_2/h_1 = 5$					
0.0	0.994	0.994	0.961	0.960	0.900	0.896
0.1	0.989	0.989	0.956	0.956	0.899	0.892
0.2	0.975	0.976	0.941	0.942	0.884	0.882
0.3	0.958	0.961	0.922	0.925	0.864	0.865
0.4	0.940	0.945	0.902	0.910	0.842	0.851
0.5	0.919	0.927	0.880	0.895	0.817	0.835
0.6	0.886	0.898	0.846	0.868	0.780	0.809
0.7	0.829	0.844	0.786	0.815	0.720	0.759
0.8	0.746	0.766	0.698	0.734	0.635	0.682
0.9	0.646	0.670	0.611	0.657	0.554	0.616

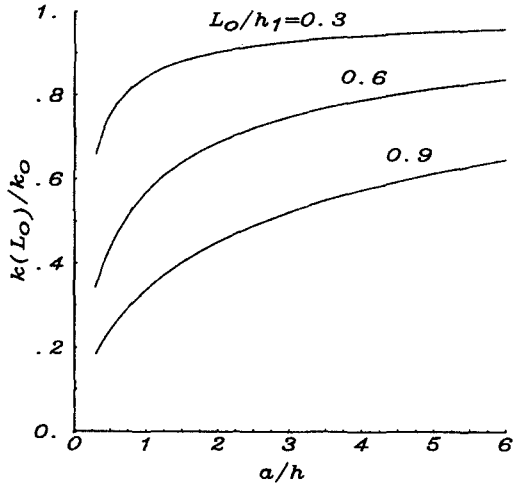

Fig. 3. The normalized stress factor at the maximum penetration point of a semi-elliptic surface crack in a two-layer orthotropic laminate under membrane loading N_0. $k_0 = k_{0t}$, $k(L_0) = k_t(0)$, $h_1 = h_2$, Material Pair *B*.

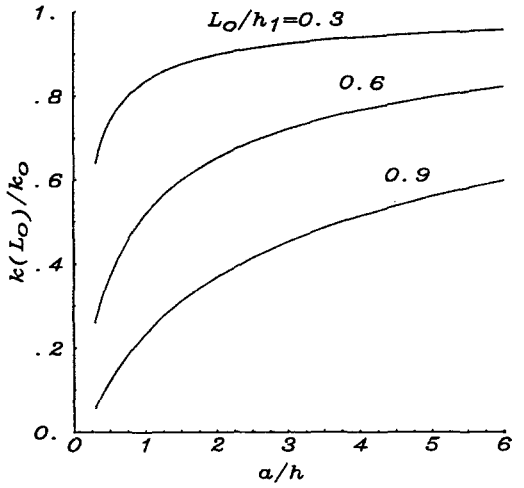

Fig. 4. The normalized stress factor at the maximum penetration point of a semi-elliptic surface crack in a two-layer orthotropic laminate under bending. $k_0 = k_{0b}$, $k(L_0) = k_b(0)$, $h_1 = h_2$, Material Pair *B*.

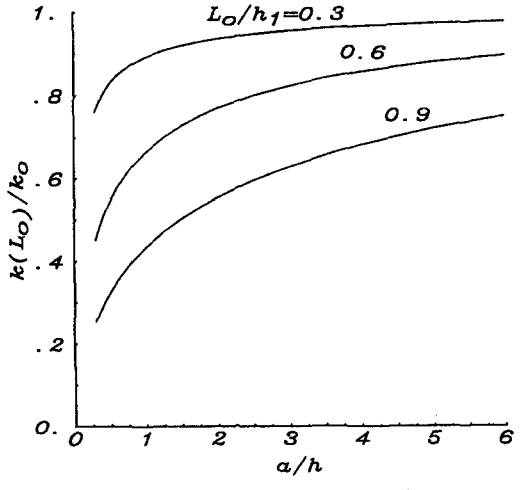

Fig. 5. Same as Fig. 3, Material Pair *I*.

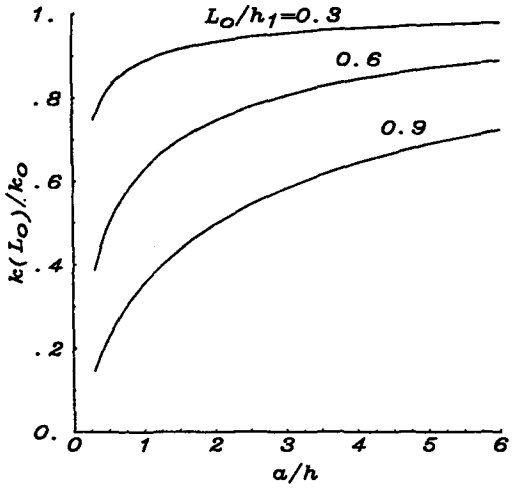

Fig. 6. Same as Fig. 4, Material Pair *I*.

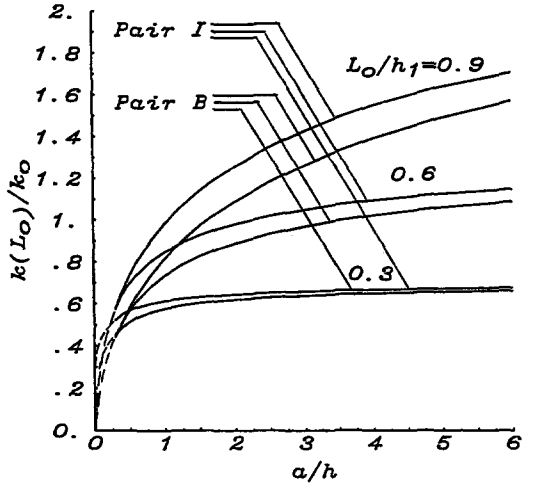

Fig. 7. Comparison of normalized stress intensity factors at the maximum penetration point of a semi-elliptic surface crack in a two-layer laminate subjected to tension for Materials *B* and *I*. $k_0 = (N_0/h)\sqrt{h_1}$, $h_1 = h_2$, $k(L_0) = k_t(0)$.

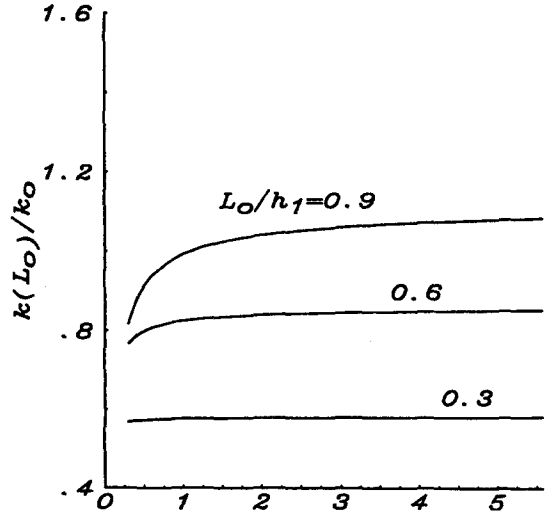

Fig. 8. The normalized stress intensity factor at the maximum penetration point of a semi-elliptic surface crack in a two-layer orthotropic laminate under membrane loading N_0, $k(L_0) = k_t(0)$, $k_0 = (N_0/h)\sqrt{h_1}$, $h_1 = 0.1\ h_2$, Material Pair *B*.

Finally Fig. 8 shows the normalized stress intensity factor at $y = 0$ for an orthotropic laminate having a thickness ratio $h_2/h_1 = 10$ and containing a semi-elliptic surface crack. Note that for $a/h > 1$ the aspect ratio $2a/L_0$ of the cracks in these examples is very large and as a/h increases $k_t(0)$ rapidly converges to its asymptotic value k_{0t}. More extensive results giving the stress intensity factors for surface cracks in orthotropic and isotropic laminates may be found in Wu (1990).

Acknowledgements—This research was supported by NSF under Grant MSS-8917867 and by NASA-Langley under Grant NAG-1-713.

REFERENCES

Erdogan, F. (1978). Mixed boundary value problems in mechanics. In *Mechanics Today* (Edited by S. Nemat-Nasser), Vol. 4, pp. 1–85. Pergamon Press, Oxford.

Erdogan, F. and Aksel, B. (1988). Line spring model and its applications to part-through crack problems in plates and shells. In *Fracture Mechanics: Nineteenth Symposium* (Edited by T. A. Cruse), pp. 125–152. ASTM, PA.

Erdogan, F. and Boduroglu, H. (1984). Surface cracks in a plate of finite width under extension or bending. *Theoret. Appl. Fract. Mech.* **2,** 197–216.

Heliot, J., Labbens, R. C. and Pellisier-Tanon, A. (1979). Semi-elliptical cracks in a cylinder subjected to stress gradients. *Fract. Mech.* pp. 341–364.

Isida, M., Noguchi, H. and Yoshida, T. (1984). Tension and bending of finite thickness plates with a semi-elliptical surface crack. *Int. J. Fract. Mech.* **26,** 157–188.

Joseph, P. F. and Erdogan, F. (1989). Surface crack problems in plates. *Int. J. Fract.* **41,** 105–131.

Joseph, P. F. and Erdogan, F. (1991a). Bending of a thin Reissner plate with a through crack. *ASME J. Appl. Mech.* **58,** 842–846.

Joseph, P. F. and Erdogan, F. (1991b). Surface crack in a plate under antisymmetric loading conditions. *Int. J. Solids Structures* **27,** 725–750.

Knowles, J. K. and Wang, N. M. (1960). On the bending of an elastic plate containing a crack. *J. Math. Phys.* **39,** 223–231.

Mattheck, C., Morawietz, P. and Munz, D. (1985). Stress intensity factor at the surface and at the deepest point of semi-elliptical surface crack in plates under stress gradients. *Int. J. Fract. Mech.* **22,** 201–212.

Newman, J. C., Jr (1978). A review and assessment of the stress-intensity factors for surface cracks. NASA Technical Memorandum 78805.

Newman, J. C., Jr and Raju, I. S. (1979). Analysis of surface cracks in finite plates under tension or bending loads. NASA Technical Paper 1578.

Nishioka, T. and Atluri, S. N. (1982). Analytical solution for embedded elliptical cracks and finite element alternating method for elliptical surface cracks subjected to arbitrary loadings. *Engng Fract. Mech.* **17,** 247–268.

Rice, J. R. and Levy, N. (1972). The part-through surface crack in an elastic plate. *ASME J. Appl. Mech.* **39,** 185–194.

Scott, P. M. and Thorpe, T. W. (1981). A critical review of crack tip stress intensity factors for semi-elliptical cracks. *Fatigue Engng Mater. Struct.* **4,** 101–114.

Shah, R. C. and Kobayashi, A. S. (1972). On the surface flaw problem. In *The Surface Crack: Physical Problems and Computational Solutions* (Edited by J. L. Swedlow), pp. 79–124. ASME, New York.

Smith, F. W. and Sorensen, D. R. (1976). The semi-elliptical surface crack—a solution by the alternating method. *Int. J. Fract. Mech.* **12,** 47–57.

Wu, B. (1990). The surface and through crack problems in layered orthotropic plates. Ph.D. Dissertation, Lehigh University.

Wu, B. and Erdogan, F. (1989). The surface and through crack problems in orthotropic plates. *Int. J. Solids Structures* **25,** 167–188.

Yahsi, O. S. and Erdogan, F. (1983). A cylindrical shell with an arbitrarily oriented crack. *Int. J. Solids Structures* **19,** 955–972.